

Tracking Control for Polysolenoid Linear Motor Base-On Model Predictive Controller: A Comparative Study of Finite Control Set and Continuous Control Set

Nguyen Hong Quang

Thai Nguyen University of Technology, 666, 3/2 Street, Tich Luong Ward, Thai Nguyen City 251750, Vietnam.

Article History: Received: 10 January 2021; Revised: 12 February 2021; Accepted: 27 March 2021; Published online: 4 June 2021

Abstract: In this paper, two predictive control methods, namely continuous control set MPC (CCS-MPC) and finite control set MPC (FCS - MPC), are applied to control Polysolenoid linear motors. These two approaches are based on the assumption that the voltage applied to the two windings on the stator of the motor is continuous or discontinuous. The method of choosing an objective function to ensure that the optimal problem always has a solution is also considered in both cases. Next, the prediction range guaranteeing the balance between the computing capability of the microcontroller and the advantages of each method is discussed. Finally, simulation results evaluate the system response to compare the performance of the two methods.

Key words: Polysolenoid Linear Motor, FCS-MPC, CCS-MMPC, MPC, PLM.

1. Introduction

Polysolenoid motors with a tubular structure are used to create direct linear motion without intermediate mechanical mechanisms such as belts, screws, etc. This makes it possible for systems using linear motors to achieve high efficiency by eliminating individual oscillations of intermediate components. The working principle of the Polysolenoid motor is presented in [1-15]. For linear motors in general, the issue of concern is the responsiveness of position accuracy. This is also an issue that has attracted the attention of many researchers. The PID controller is applied in [16] with the advantage of a simple control design but not responding to the internal noise of the system. To improve the efficiency of the PID controller, the research in [17] combined PID with an iterative learning algorithm to improve the position accuracy in the repetitive operation of industrial robots. A linear motor is a nonlinear object represented in the model structure. In addition, the external disturbance is also an unpredictable component that affects the control quality of the system. To deal with external disturbance involving the system, the sliding control method [18-22] is a commonly applied method. These methods are particularly effective with friction disturbance because it is a factor that cannot be modeled precisely. In [18], a sliding surface with a fixed response time is performed to drive the system state to convergence after a fixed time interval. Super-twisting sliding mode is used in [19], achieving a good effect with the impact of the external disturbances on the system through experimental results. In [20], a sliding controller combined with an adaptive disturbance observer is applied to the PLMSM. In this study, the stability is proven according to Lyapunov, and the position error converges to zero in a finite time. Discrete-time fast terminal sliding mode is used in [21] to improve the steady-state performance of the system. In [22], the adaptive fractional order (FO) terminal sliding mode control is applied to PLMSM with the advantage that the sign function does not exist in the switching input, thus limiting the chattering behavior of the sliding control method.

From the above analysis, we see that the sliding control method can deal with disturbances and reduce the computation time of the controller, which is especially significant for systems where the processing capacity of the microprocessor is limited. Currently, the technology of manufacturing microcontrollers has developed tremendously, making it possible for us to apply complex control algorithms to motor drives in the industry. That is why model predictive control (MPC) for electric motors has begun to be exploited. Recently, MPC has been started to be applied to control electric drive systems and power electronic systems. Studies on MPC have successfully implemented speed control with rotary motors [23-25]. The characteristic of MPC is that it requires a large amount of computation because it is involved in selecting the prediction range when applied. With the MPC implemented for Polysolenoid motors, the precise response of the inner loop with sampling time is often smaller than that of the outer loop. The effect is that the system can achieve the exact position according to the reference value when the outer loop controller is just a PI controller.

2. Mathematical Model of Polysolenoid Motors

The structure of the Polysolenoid motor is shown in Figure 1. The two windings of the motor are powered by a two-phase voltage source inverter, depicted in Figure 2.

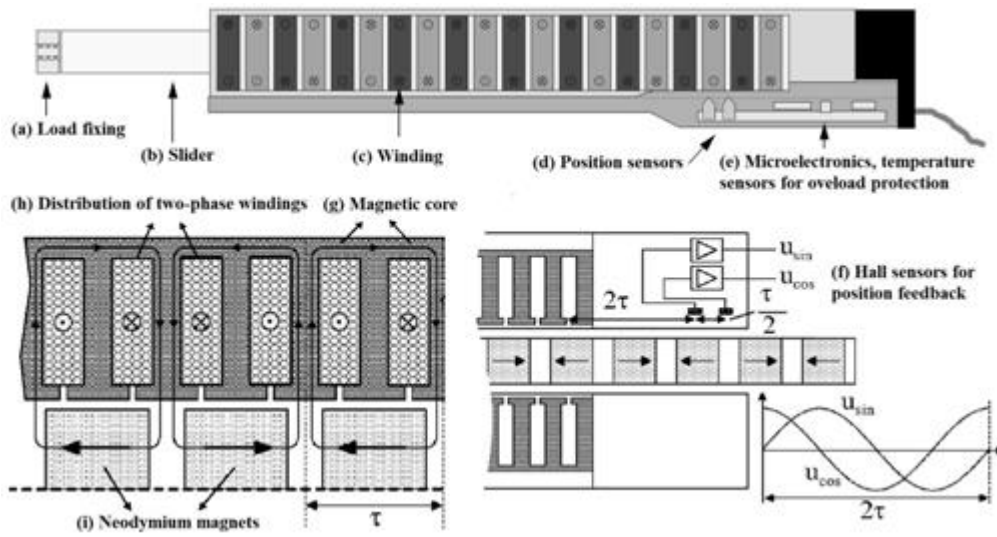


Figure 1: Polysolenoid Motor [1,3]

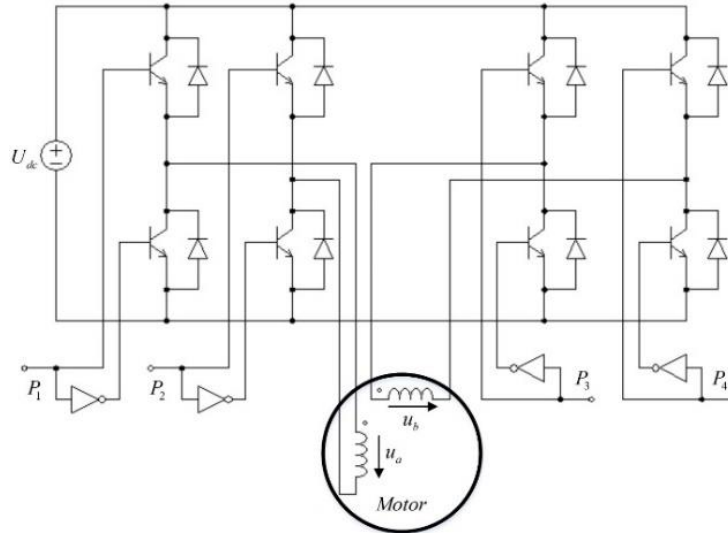


Figure 2: Structure of the Voltage Source Inverter for Polysolenoid Motor.

The mathematical model of Polysolenoid motor on the dq -coordinate system is as below [8]:

$$\begin{cases} \frac{di_{sd}}{dt} = -\frac{R_s}{L_{sd}} i_{sd} + \left(\frac{2\pi p}{\tau} v\right) \frac{L_{sq}}{L_{sd}} i_{sq} + \frac{u_{sd}}{L_{sd}} \\ \frac{di_{sq}}{dt} = -\frac{R_s}{L_{sq}} i_{sq} - \left(\frac{2\pi p}{\tau} v\right) \frac{L_{sd}}{L_{sq}} i_{sd} - \left(\frac{2\pi p}{p\tau} v\right) \frac{\psi_p}{L_{sq}} + \frac{u_{sq}}{L_{sq}} \\ \frac{dv}{dt} = \frac{2\pi p}{\tau} (\psi_p + (L_{sd} - L_{sq}) i_{sd}) i_{sq} - \frac{1}{m} F_c \\ \frac{dx}{dt} = v \end{cases} \quad (1)$$

From (1), the continuous current model of the Polysolenoid motor on the dq -coordinate system is driven as:

$$\frac{d\mathbf{i}_{dq}}{dt} = \mathbf{A}\mathbf{i}_{dq} + \mathbf{B}\mathbf{u}_{dq} + \mathbf{N}\mathbf{i}_{dq}\omega_e + \mathbf{S}\psi_p\omega_e \quad (2)$$

Where

$$\mathbf{i}_{dq}^T = [i_d \quad i_q], \mathbf{u}_{dq}^T = [u_d \quad u_q]$$

$$\mathbf{A} = \begin{bmatrix} -\frac{R_s}{L_d} & 0 \\ 0 & -\frac{R_s}{L_q} \end{bmatrix}, \mathbf{B} = \begin{bmatrix} \frac{1}{L_d} & 0 \\ 0 & \frac{1}{L_q} \end{bmatrix}, \mathbf{N} = \begin{bmatrix} 0 & \frac{L_q}{L_d} \\ -\frac{L_d}{L_q} & 0 \end{bmatrix}, \mathbf{S} = \begin{bmatrix} 0 \\ -\frac{1}{L_q} \end{bmatrix}$$

- A** System matrix.
B Input matrix.
N Non-linear compound matrix.
S Noise matrix.

3. Control Design

From the continuous model, we can determine the discrete-time model of the stator current as below:

$$\mathbf{i}_{dq}(k+1) = \mathbf{\Phi} \mathbf{i}_{dq}(k) + \mathbf{H} \mathbf{u}_{dq}(k) + \mathbf{h} \psi_p \quad (3)$$

in which

$$\mathbf{\Phi} = \mathbf{I} + T_s \mathbf{A} + T_s \mathbf{N} \omega_e(k) = \begin{bmatrix} \Phi_{11} & \Phi_{12} \\ \Phi_{21} & \Phi_{22} \end{bmatrix} = \begin{bmatrix} 1 - T_s R_s / L_d & T_s L_q \omega_e(k) / L_d \\ -T_s L_d \omega_e(k) / L_q & 1 - T_s R_s / L_q \end{bmatrix}$$

$$\mathbf{H} = T_s \mathbf{B} = \begin{bmatrix} H_{11} & 0 \\ 0 & H_{22} \end{bmatrix} = \begin{bmatrix} T_s / L_d & 0 \\ 0 & T_s / L_q \end{bmatrix}, \mathbf{h} = \begin{bmatrix} h_1 \\ h_2 \end{bmatrix} = \begin{bmatrix} 0 \\ -T_s \omega_e(k) / L_q \end{bmatrix}$$

Where T_s is the sampling time of the current.

Based on the discrete-time model, we build a predictive model with $\mathbf{i}_{dq}^{est}(k+i)$ is the predicted current value at the next i -th sample compared to the current time. From (3), we have:

$$\mathbf{i}_{dq}^{est}(k+i+1|k) = \mathbf{\Phi} \mathbf{i}_{dq}^{est}(k+i|k) + \mathbf{H} \bar{\mathbf{u}}_{dq}(k+i) + \mathbf{h} \psi_p \quad (4)$$

In which at the current time k : $\mathbf{i}_{dq}^{est}(k) = \mathbf{i}_{dq}(k)$, $\bar{\mathbf{u}}_{dq}(k+i)$ denotes the control signal at the next i -th sample. The intended use of $\bar{\mathbf{u}}_{dq}$ is to distinguish it from the actual control signals applied to the system $\mathbf{u}_{dq}(k), \mathbf{u}_{dq}(k-1)$, etc. With the prediction range N_p , the MPC solves the optimization problem in which control voltage vectors $\bar{\mathbf{u}}_{dq}(k) = \mathbf{u}_{dq}(k), \bar{\mathbf{u}}_{dq}(k+1), \dots, \bar{\mathbf{u}}_{dq}(k+N_p-1)$ are variables.

The objective function of the optimization problem can be chosen arbitrarily, but the solution does not always exist for the chosen objective function. To solve the problem that the objective function may not have a solution in some cases, we choose the selected objective function of the following quadratic form:

$$J = \sum_{i=1}^{N_p} \left[\left(\mathbf{i}_{dq}^{ref} - \mathbf{i}_{dq}^{est}(k+i|k) \right)^T \mathbf{Q} \left(\mathbf{i}_{dq}^{ref} - \mathbf{i}_{dq}^{est}(k+i|k) \right) \right] \quad (5)$$

Where $\mathbf{Q} = \text{diag}([\lambda_d \quad 1])$ is a positive definite diagonal matrix, λ_d is the coefficient representing the weight of the current deviation from $|i_d^{ref} - i_d|$ to $|i_q^{ref} - i_q|$ in the objective function J , \mathbf{i}_{dq}^{ref} is the reference signal coming from the output of the speed controller.

Due to the fast current-driven loop kinematics, the prediction range N_p is chosen to be small in order to reduce the computational weight in (5), ensuring the performance of the controller. In addition, in industrial applications, the sampling cycle of the current loop is many times faster than that of the speed loop. Combining the above reasons, we can consider the speed and angular position of the motor to be constant during one sampling cycle resulting in the constant \mathbf{i}_{dq}^{ref} in Equation (5).

Select the Objective Function with the CCS-MPC Method

With the CCS-MPC method, we consider the voltage supplied to the two windings of the motor to be continuous. Due to the limitation on modulation, the voltage will be in a bounded, continuous set. The modulation domain with the CCS-MPC method is shown in Figure 3.

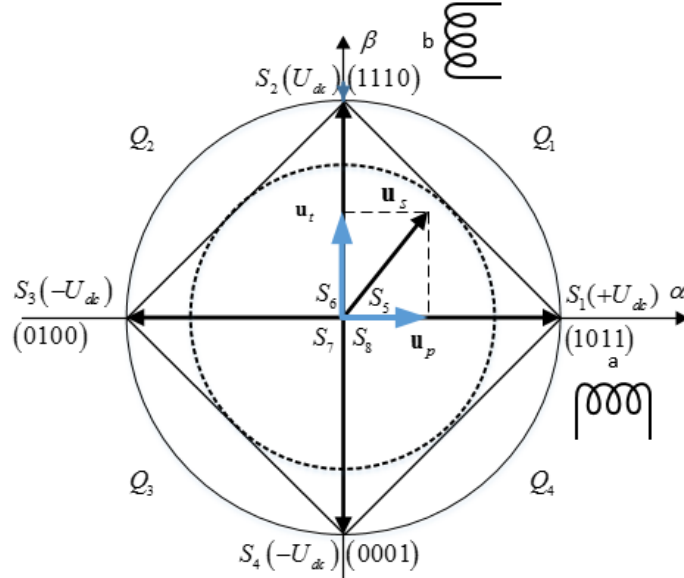


Figure 3: Modulation Plane on the $\alpha\beta$ -Coordinate System with the CCS-MPC.

From (5), considering the particular case with the continuous modulation domain, we choose the prediction range N_p .

To reduce the computation time for the current control loop, we choose the prediction range $N_p = 1$. The optimization problem (5) with the function is transformed to the quadratic form with $\bar{\mathbf{u}}_{dq}(k) = \mathbf{u}_{dq}(k)$ is the optimal variable as follows:

$$\min_{\bar{\mathbf{u}}_{dq}(k)} J = \bar{\mathbf{u}}_{dq}(k)^T (\mathbf{H}^T \mathbf{Q} \mathbf{H}) \bar{\mathbf{u}}_{dq}(k) + 2(\Phi \mathbf{i}_{dq}(k) + \mathbf{h} \psi_p - \mathbf{i}_{dq}^{ref})^T \mathbf{Q} \mathbf{H} \bar{\mathbf{u}}_{dq}(k) + C \quad (6)$$

$$\text{Subject to: } \mathbf{A}_{con} \mathbf{R}^{-1} \bar{\mathbf{u}}_{dq}(k) < \mathbf{B}_{con}$$

Where C is the component that depends only on the current state and the current velocity, not on $\mathbf{u}_{dq}(k)$. Solving the optimization problem by QP (quadratic programming) method, we obtain the required voltage value $\mathbf{u}_{dq}(k)$.

Select the Objective Function with FCS-MPC Method

The disadvantage of the CCS-MPC method is that solving the maximal problem requires a lot of computation time, even though the solution that minimizes the most computational time is selected, i.e., $N_p = 1$.

For objects with discontinuous nature, such as power converters, the FCS-MPC method is very effective. This method is based on a finite number of possible valve combinations of the power converter. The FCS-MPC optimization problem can be easily solved by a finite number of iterations. However, the number of these loops will increase exponentially with the prediction range. This leads to a significant increase in computation time and loss of the advantage of the method.

With the FCS-MPC method, the prediction range is selected as $N_p = 2$. Then the objective function has the following form

$$\begin{aligned} \min_{\bar{\mathbf{u}}_{dq}(k), \bar{\mathbf{u}}_{dq}(k+1)} J = & \bar{\mathbf{u}}_{dq}(k)^T (\mathbf{H}^T \mathbf{Q} \mathbf{H}) \bar{\mathbf{u}}_{dq}(k) + \bar{\mathbf{u}}_{dq}(k+1)^T (\mathbf{H}^T \mathbf{Q} \mathbf{H}) \bar{\mathbf{u}}_{dq}(k+1) \\ & + \bar{\mathbf{u}}_{dq}(k)^T (\mathbf{H}^T \mathbf{Q}^T \mathbf{Q} \mathbf{H}) \bar{\mathbf{u}}_{dq}(k+1) \\ & + 2(\Phi \mathbf{i}_{dq}(k) + \mathbf{h} \psi_p - \mathbf{i}_{dq}^{ref})^T \mathbf{Q} \mathbf{H} \bar{\mathbf{u}}_{dq}(k) \\ & + 2(\Phi^2 \mathbf{i}_{dq}(k) + \Phi \mathbf{h} \psi_p - \mathbf{i}_{dq}^{ref})^T \mathbf{Q} \mathbf{H} \bar{\mathbf{u}}_{dq}(k+1) \end{aligned} \quad (7)$$

$$\text{subject to: } \bar{\mathbf{u}}_{dq} \in \mathbf{U} \square \{ \mathbf{R} \mathbf{u}_{s_1}, \mathbf{R} \mathbf{u}_{s_2}, \mathbf{R} \mathbf{u}_{s_3}, \mathbf{R} \mathbf{u}_{s_4}, \dots, \mathbf{R} \mathbf{u}_{s_n}, \mathbf{u}_0 \}$$

Where \mathbf{u}_{S_i} is the stator voltage vector generated by the switching state S_i , \mathbf{u}_0 is the zero voltage vector, \mathbf{i}_{dq}^{ref} is the reference current vector, S_i are the basis vectors formed by the fixed valve opening and closing combination. These basis vectors are shown in Figure 4.

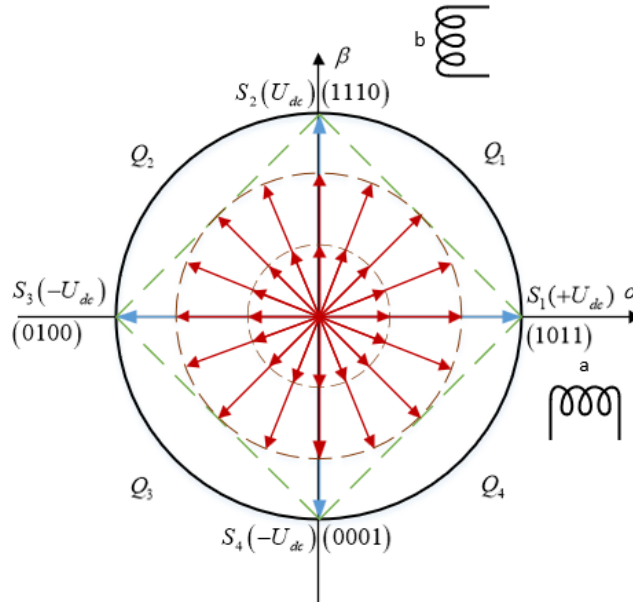


Figure 4: The Basis Vectors used in the FCS-MPC Method.

4. Simulation Results

To find out the level of awareness on healthy dietary habits among prospective teachers. The motor parameters are described in Table. 1.

Table 1: Motor Parameters

| Motor Parameters | Symbol | Value | Unit |
|--------------------------|----------|-------|----------|
| d axis stator inductance | L_{sd} | 1.4 | mH |
| q axis stator inductance | 34 | 1.4 | mH |
| Stator resistance | L_{sq} | 10.3 | Ω |
| Rotor flux | ψ_p | 0.035 | Wb |
| Number of pole pair | z_p | 2 | |
| Pole step | τ_p | 0.02 | m |

System simulation is performed in two cases:

Case 1: Simulate the response of FCS-MPC and CCS-MPC current regulators to the change in the reference of the current loop. The initial reference current is 0.25A. Then this value increases to 0.5A at $t = 0.5s$.

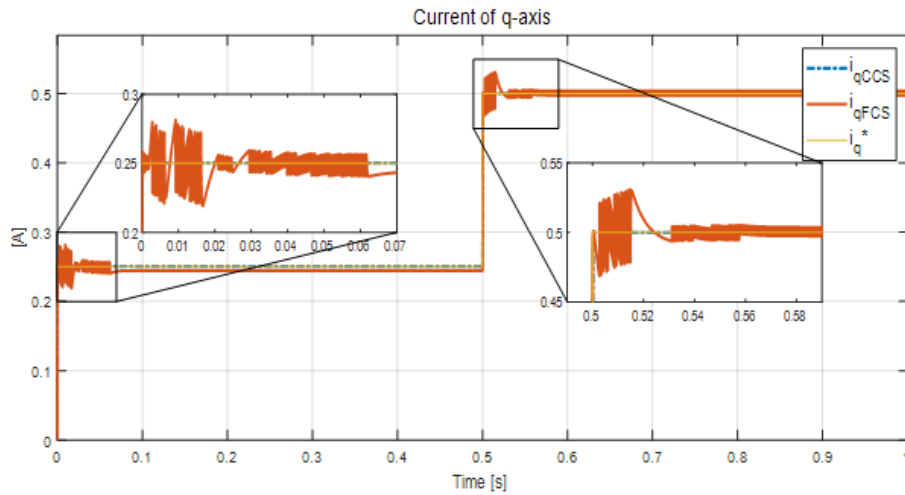


Figure 5: q-Axis Current Response.

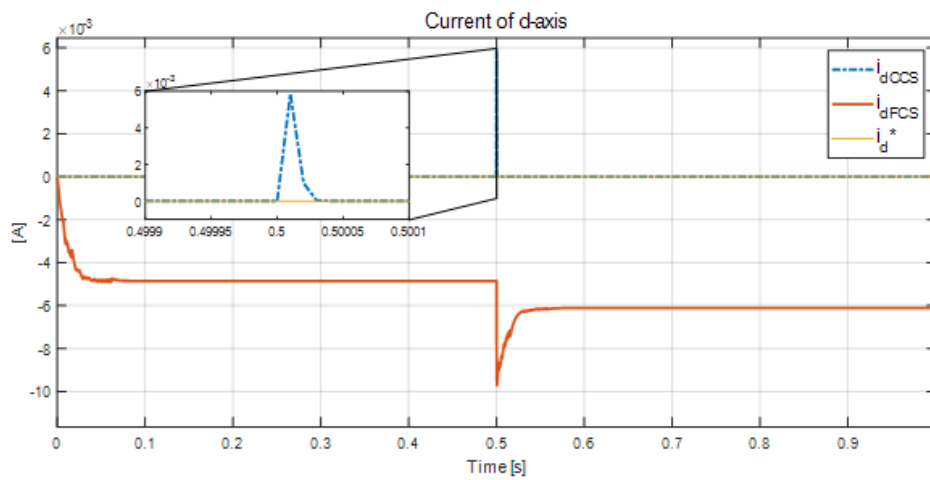


Figure 6: d-Axis Current Response.

Comment: When changing the reference current value i_q , the current responses on d- and q- axes are shown in Figure 6 and Figure 7. The q-axis currents of both CCS-MPC and FCS-MPC methods track to the reference value, as shown in Figure 6. With the CCS-MPC method, the response current tracks to the reference value without an overshoot. The response current value of the FCS-MPC method still has a small amount of overshoot. Besides, the smoothness of the current of the FCS-MPC method is worse than that of the CCS-MPC method.

From the response of the d-axis current, as depicted in Figure 7, we can see that there is still a current deviation with the FCS-MPC method. However, the value of this deviation is acceptable. This is because, with the FCS-MPC method, the basis vector with the closest value is selected after each optimization problem. Therefore, it may not coincide with the vector that the CCS-MPC method needs to modulate with the solution of the optimization problem in the objective function.

Case 2: Simulate system position response with FCS-MPC and CCS-MPC current controllers. The outer loop controller has the parameters given by Table.2.

Table 2: Control Parameters

| Control Parameters | Symbol | Controller |
|----------------------------------------------|---------------|------------|
| Proportional gain of the position controller | k_{pp} | 40 |
| Proportional gain of the speed controller | $k_{p\omega}$ | 0.1 |
| Integral gain of the speed controller | $k_{i\omega}$ | 10 |

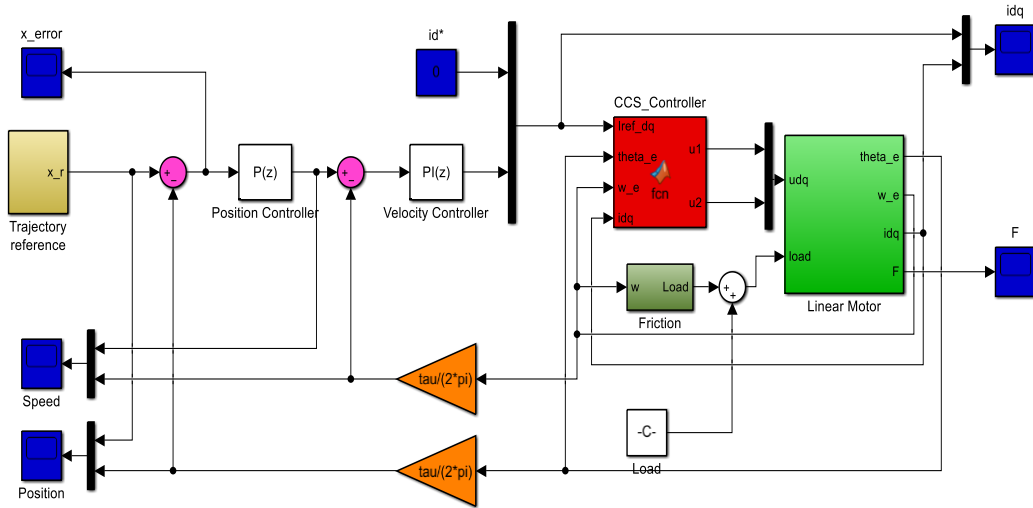


Figure.7 Control Structure of the System with CCS-MPC Method.

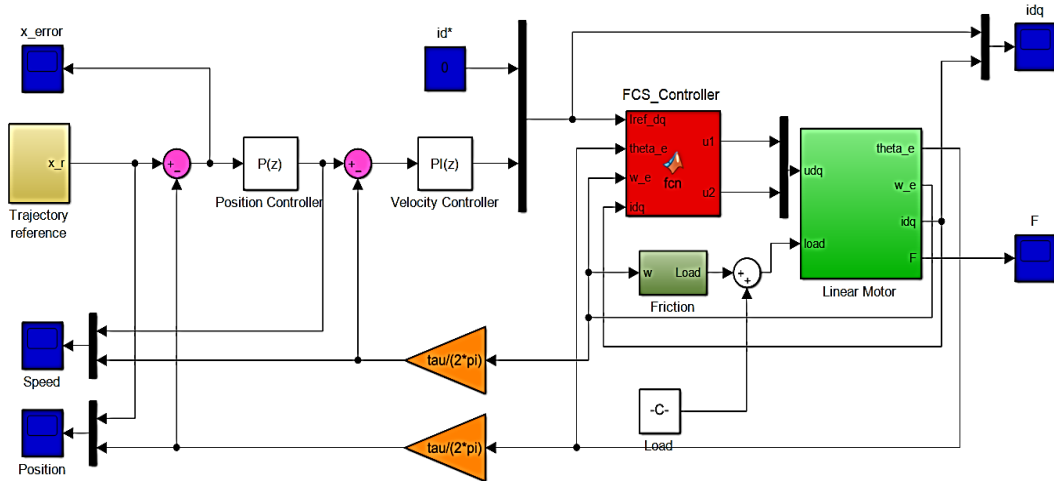


Figure 8: Control Structure of the System with FCS- MPC Method.

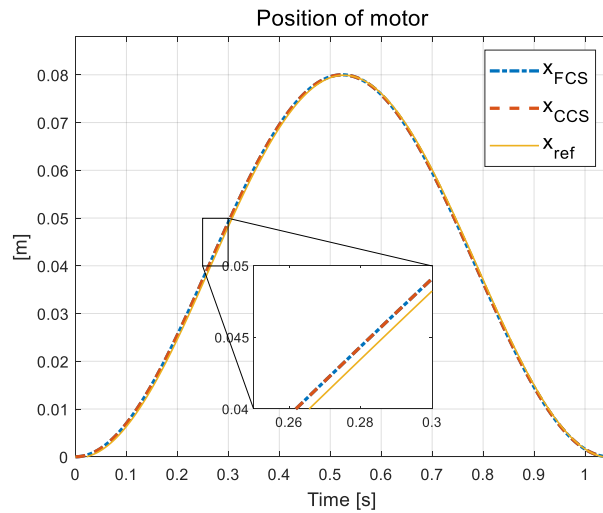


Figure 9: Position Response.

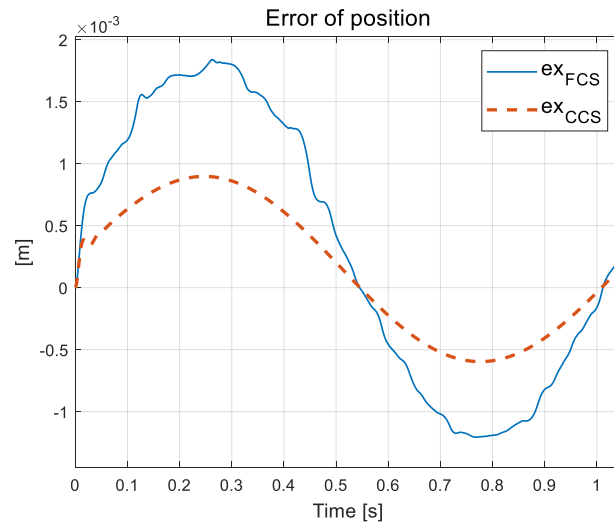


Figure 10: Position Error.

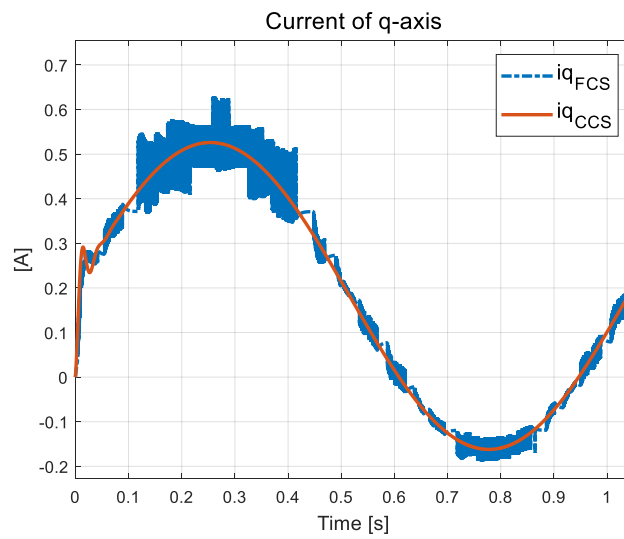


Figure 11: q-Axis Current Response.

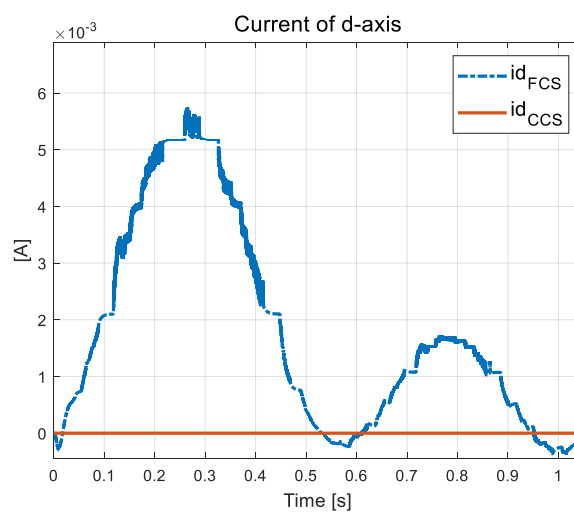


Figure 12: d-Axis Current Response.

Comments: When the thrust loop achieves fast and precise kinematics, a simple PI-type controller can be selected in the outer loop while still responding to the position accurately. When the thrust loop achieves fast and accurate kinematics, we can choose a simple PI controller in the outer loop that can still satisfy the precise response of the position. In the position control problem with two methods of designing thrust loops, CCS-MPC and FCS-MPC, the response value follows the exact reference value, as shown in Figure 10. From the results of position deviation and current response on d- and q- axes, as shown in Figures 10, 11, 12, we see that the CCS-MPC method gives better results than the FCS-MPC method. With the FCS-MPC method, the smoothness of the current is not as good as that of the CCS-MPC method. This is reasonable since the basis vector set of the FCS-MPC method is finite. The control designer sets this number of vectors, and we can actively change this number of base vectors to improve the smoothness of the current.

5. Conclusions

This paper has designed a controller for Polysolenoid motor using CCS-MPC and FCS-MPC methods. We can choose one of two methods that meet the output quality requirements from the power requirements, quality, and hardware constraints. Some typical properties of the FCS-MPC method that can replace CCS-MPC when limited in the processing capacity of the integrated microprocessor in the system are as below:

- Based on the discontinuous nature of the voltage applied to the motor through the converter, the FCS MPC can completely ignore the vector modulation compared to the CCS-MPC if the selected finite vector set coincides with the base vector set. Thus, the computational weight of the controller is reduced.
- Because the finite vector set is predetermined, the FCS-MPC method does not have to determine the modulation limit domain into account as for the CCS-MPC. This is important in some converters with complex modulation domains.
- The optimization problem using FCS-MPC always has a solution because the domain of the optimal variables is finite, and the solution time is short. In addition, the objective function is not necessarily of the quadratic form. In addition, with a nonlinear object model, the FCS method can still be solved quickly, while the MPC CCS method becomes less efficient because the objective function is not of the quadratic form.

There is a feature we can notice, with the FCS-MPC method, when the selected base vector set increases to fill the modulation domain, it will become the CCS-MPC method.

Acknowledgments

This research was funded by Thai Nguyen University of Technology, No. 666, 3/2 street, Thai Nguyen, Viet Nam.

References

1. Ausderau, D. (2004). Polysolenoid-Linearantrieb mit genutetem Stator (Doctoral dissertation, ETH Zurich).
2. Boldea, I. (2013). Linear electric machines, drives, and MAGLEVs handbook. CRC press.
3. LinMot Company Home Page: Products, Linear Motors. Available online: <https://linmot.com/products/linear-motors/> (accessed on 1 March 2020).
4. Gieras, J. F. (2002). Permanent magnet motor technology: design and applications. CRC press.
5. Nguyen, Q. H., Dao, N. P., Nguyen, T. T., Nguyen, H. M., Nguyen, H. N., & Vu, T. D. (2016). Flatness based control structure for polysolenoid permanent stimulation linear motors. SSRG International Journal of Electrical and Electronics Engineering, 3(12), 31-37.
6. Quang, N. H. (2017). Multi parametric programming based model predictive control for tracking control of polysolenoid linear motor. Special issue on Measurement, Control and Automation, 19, 31-37.
7. Nguyen, H. Q. (2020, March). Observer-Based Tracking Control for Polysolenoid Linear Motor with Unknown Disturbance Load. In Actuators (Vol. 9, No. 1, p. 23).
8. Quang, N. H., Quang, N. P., & Hien, N. N. (2020). On tracking control problem for polysolenoid motor model predictive approach. International Journal of Electrical & Computer Engineering (2088-8708), 10(1).
9. Nam, D. P., Quang, N. H., Hung, N. M., & Ty, N. T. (2017, July). Multi parametric programming and exact linearization based model predictive control of a permanent magnet linear synchronous motor. In 2017 International Conference on System Science and Engineering (ICSSE) (pp. 743-747). IEEE.
10. Ty, N. T., Hung, N. M., Nam, D. P., & Quang, N. H. (2018). A Laguerre model-based model predictive control law for permanent magnet linear synchronous motor. In Information Systems Design and Intelligent Applications (pp. 304-313). Springer, Singapore.

11. Quang, N. H., Quang, N. P., Nam, D. P., & Binh, N. T. (2019). Multi parametric model predictive control based on laguerre model for permanent magnet linear synchronous motors. *International Journal of Electrical and Computer Engineering (IJECE)*, 9(2), 1067-1077.
12. Nguyen, H. Q., Nguyen, P. Q., Nguyen, N. H., & Nguyen, T. B. (2018). Min max model predictive control for polysolenoid linear motor. *International Journal of Power Electronics and Drive Systems*, 9(4), 1666.
13. Higuchi, T., Nonaka, S., & Ando, M. (2001). On the design of high-efficiency linear induction motors for linear metro. *Electrical Engineering in Japan*, 137(2), 36-43.
14. Lu, H., Zhu, J., & Guo, Y. (2005, July). A tubular linear motor for micro robotic applications. In *IEEE International Conference on Mechatronics, 2005. ICM'05.* (pp. 596-601). IEEE.
15. Li, L., Xuzhen, H., Donghua, P., & Jiwei, C. (2010). Magnetic field of a tubular linear motor with special permanent magnet. *IEEE Transactions on Plasma Science*, 39(1), 83-86.
16. Şumnu, A., Güzelbey, İ. H., & Çakir, M. V. (2017). Simulation and PID control of a Stewart platform with linear motor. *Journal of mechanical science and technology*, 31(1), 345-356.
17. Li, H., Sheng, H., & Shen, L. (2021, April). Iterative learning PID Controller for Permanent Magnet Linear Synchronous Motor. In *Journal of Physics: Conference Series (Vol. 1852, No. 3, p. 032044).* IOP Publishing.
18. Li, J., Du, H., Cheng, Y., Wen, G., Chen, X., & Jiang, C. (2019). Position tracking control for permanent magnet linear motor via fast nonsingular terminal sliding mode control. *Nonlinear Dynamics*, 97(4), 2595-2605.
19. Li, Z., Zhou, S., Xiao, Y., & Wang, L. (2019). Sensorless vector control of permanent magnet synchronous linear motor based on self-adaptive super-twisting sliding mode controller. *IEEE Access*, 7, 44998-45011.
20. Shao, K., Zheng, J., Wang, H., Xu, F., Wang, X., & Liang, B. (2021). Recursive sliding mode control with adaptive disturbance observer for a linear motor positioner. *Mechanical Systems and Signal Processing*, 146, 107014.
21. Du, H., Chen, X., Wen, G., Yu, X., & Lü, J. (2018). Discrete-time fast terminal sliding mode control for permanent magnet linear motor. *IEEE Transactions on Industrial Electronics*, 65(12), 9916-9927.
22. Sun, G., & Ma, Z. (2017). Practical tracking control of linear motor with adaptive fractional order terminal sliding mode control. *IEEE/ASME Transactions on Mechatronics*, 22(6), 2643-2653.
23. Wróbel, K., Serkies, P., & Szabat, K. (2020). Model Predictive Base Direct Speed Control of Induction Motor Drive—Continuous and Finite Set Approaches. *Energies*, 13(5), 1193.
24. Sahu, A., Mohanty, K. B., & Mishra, R. N. (2021, January). Design of MPC-PSO based Torque Regulator for DTC-SVM Induction Motor Drive. In *2021 1st International Conference on Power Electronics and Energy (ICPEE)* (pp. 1-6). IEEE.
25. Tan, K., Su, J., & Wang, H. (2020, October). MPC Based Full-speed Domain Control Strategy of Interior Permanent Magnet Synchronous Motor. In *IECON 2020 The 46th Annual Conference of the IEEE Industrial Electronics Society* (pp. 1040-1045). IEEE.